New investigation of half-lives for the decay modes of ^{50}V

M. Laubenstein,[1,*] B. Lehnert,[2,†] S. S. Nagorny,[3,‡] S. Nisi,[1,§] and K. Zuber[4,5,‖]
[1]*INFN - Laboratori Nazionali del Gran Sasso, 67100 Assergi (AQ), Italy*
[2]*Nuclear Science Division, Lawrence Berkeley National Laboratory, Berkeley, California 94720, USA*
[3]*Queen's University, Physics Department, Kingston, Ontario K7L 3N6, Canada*
[4]*Institut für Kern- und Teilchenphysik, TU Dresden, 01069 Dresden, Germany*
[5]*Magyar Tudomnyos Akadmia Atomki, 4026 Debrecen, Hungary*

(Received 14 December 2018; published 5 April 2019)

A new search for the decay modes of the fourfold forbidden nonunique decay of ^{50}V has been performed at the Gran Sasso Underground Laboratory (LNGS). In total, an exposure of 197 kg d has been accumulated. The half-life for the electron capture into the first excited state of ^{50}Ti has been measured with the highest precision to date as $2.67^{+0.16}_{-0.18} \times 10^{17}$ yr (68% C.I.) in which systematics uncertainties dominate. The search for the β decay into the first excited state of ^{50}Cr resulted in a lower limit of 1.9×10^{19} yr (90% C.I.), which is an improvement of almost one order of magnitude compared to existing results. The sensitivity of the new measurement is now in the region of theoretical predictions.

DOI: 10.1103/PhysRevC.99.045501

I. INTRODUCTION

The search for extremely rare events like dark matter, nucleon decays, or neutrinoless double beta decay is a widespread activity in particle astrophysics and in the search for physics beyond the standard model of particle physics. Such experiments are typically located underground to reduce backgrounds from cosmic rays, with further reduction of background by using materials with low radioactive contaminations. As an example, in this way the neutrino-accompanied double beta decay ($2\nu\beta\beta$ decay) has been observed for almost a dozen isotopes whose half-lives are in the region of 10^{18}–10^{24} yr.

Having achieved such a sensitivity, it is an obvious step also to study other very long-living nuclides, which typically feature highly forbidden beta decays and electron captures (ECs). It turns out that in extremely highly forbidden decays, like the fourfold forbidden unique transitions ($\Delta I^{\Delta\pi} = 5^+$) of ^{48}Ca and ^{96}Zr, single β decay and $2\nu\beta\beta$ decay compete with each other. For ^{96}Zr the β-decay half-life is calculated at 2.4×10^{20} yr [1]. The $2\nu\beta\beta$ half-life has been measured by the NEMO-3 Collaboration to be $T_{1/2} = 2.35 \pm 0.14(\text{syst.}) \pm 0.16(\text{stat.}) \times 10^{19}$ yr [2]. Single β decay has been searched for and a lower limit of $T_{1/2} > 2.4 \times 10^{19}$ yr has been given [3]. A similar case can be made for ^{48}Ca: The $2\nu\beta\beta$ decay has been measured as $T_{1/2} = 6.4^{+0.7}_{-0.6}(\text{stat.})^{+1.2}_{-0.9}(\text{syst.}) \times 10^{19}$ yr by NEMO-3 [4]. A half-life limit of the β decay to the corresponding 5^+ excited state of ^{48}Ti results in a lower limit of $T_{1/2} > 2.5 \times 10^{20}$ yr [5]. These results slightly indicate that indeed $2\nu\beta\beta$ decay is more likely than β decay in ^{48}Ca and ^{96}Zr.

The next group of nuclides, with one unit of spin change less, have fourfold forbidden nonunique transitions ($\Delta I^{\Delta\pi} = 4^+$); this group contains isotopes like ^{113}Cd, ^{115}In, and ^{50}V, the latter being explored in this paper.

The isotope ^{50}V is quite special in the sense that in contrast to ^{113}Cd and ^{115}In the ground state transition is even more highly forbidden, leaving only fourfold forbidden nonunique decay modes into the first excited state of ^{50}Cr and ^{50}Ti, both characterized as $6^+ \rightarrow 2^+$ transitions. The ground state transitions to both isotopes are even sixfold forbidden nonunique decays. The decay scheme is shown in Fig. 1.

The Q value for the β decay into ^{50}Cr is ($Q_\beta = 1038.06 \pm 0.30$) keV and for electron capture (EC) into ^{50}Ti it is ($Q_{EC} = 2207.6 \pm 0.4$) keV [6]. There is only one excited state in each daughter nucleus which can be populated. The corresponding γ lines to search for are 1553.77 keV for EC into the first excited state of ^{50}Ti and 783.29 keV for the β decay into the first excited state of ^{50}Cr . The photon emission probability of both $E2$ transitions is 1 (with a negligible uncertainty).

The history of attempts to observe the decay of ^{50}V is quite special and has spanned more than 60 years, during which several potential detections were proved wrong by newer, more sensitive experiments. This pattern repeated several times [7–16]. Furthermore, the deduced half-life is different in different articles, while uncertainties claimed were typically well beyond 20%. The measurements within the last 45 years are compiled below in Table VII. A first clear observation of the EC-branch decay to ^{50}Ti was reported by [17]. In the meantime a first theoretical nuclear shell model calculation was performed for the β^--decay mode which predicts a half-life value of about 2×10^{19} yr [18].

*matthias.laubenstein@lngs.infn.it
†bjoernlehnert@lbl.gov
‡sn65@queensu.ca
§stefano.nisi@lngs.infn.it
‖zuber@physik.tu-dresden.de

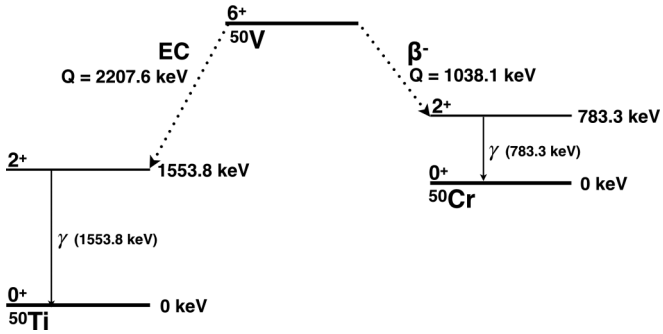

FIG. 1. Decay scheme of ^{50}V. Two excited states can be populated: one via EC to ^{50}Ti under emission of a 1553.77 keV γ ray and the other via the β decay into the first excited state of ^{50}Cr resulting in a 783.29 keV γ ray.

The aim of this paper is to perform a high statistics measurement of the EC-branch decay to ^{50}Ti and improve and explore the β-decay branch of the ^{50}V decay, taking advantage of the most sophisticated low-background detector system based on high-purity germanium (HPGe) detectors in one of the deepest underground laboratories available.

II. EXPERIMENTAL SETUP

The vanadium sample was produced from vanadium flakes by multifold electron beam melting (EBM) under high vacuum as described in detail in Ref. [19]. Vanadium with an initial purity grade of 97 wt.% was used as starting material. The small flakes of vanadium metal were compressed into tablets with dimensions of 30×10 mm (d × h) and about 35 g of mass each. The EBM purification process produced ingots with a diameter of about 45 mm, which were later cut into discs of about 40 × 10 mm (d × h).

A. Chemical purity of the vanadium sample

In order to determine the residual impurities and their concentration and to evaluate the efficiency of the refining process, several analyses have been performed. A general comparative analysis of elemental impurities in the vanadium before and after purification was carried out by laser mass spectrometry. Two samples of vanadium in the form of small plates, 5 × 5 × 3 mm^3, with chemically cleaned surfaces were analyzed.

The results are shown in Table I. As can be seen, the EBM refining method is rather effective for elements that have a high separation factor at the typical temperature for the vanadium refining process of 2400 K. For example, the Cr concentration was reduced by two orders of magnitude and K was reduced 75 times. On the other hand, for some elements (e.g., Ni, Si) almost no purification occurred. More details can be found in Ref. [19], where the separation coefficients α_i for the main impurity elements in vanadium were determined and investigated.

The gas-forming impurities were also removed with high efficiency by the EBM process. The outgassing of the vanadium samples was measured before and after purification using an MX7203 mass spectrometer [20], within a temperature range from 25 to 800 °C. Four main components are released from the vanadium samples during the thermal desorption: H_2O, CO, N_2 and CO_2. The intensity of outgassing for the sample after refining is five times less than for the starting metal. Overall, the concentration of oxygen was reduced from $(700 \pm 100) \times 10^{-6}$ g/g in the initial vanadium flakes to $(170 \pm 20) \times 10^{-6}$ g/g, which is the dominant impurity in the refined metal sample. The outgassing impurities as well as the total impurity of the vanadium sample are the lowest achieved so far. The vanadium purity is well determined at (99.97 ± 0.01) wt.% which allows us to reduce the mass uncertainty in the analysis.

TABLE I. Concentration of impurities in the vanadium sample before and after purification with electron beam melting (EBM). Values are given in units of 10^{-6} g/g with estimated uncertainty on the level of 30%.

Element	Before EBM	After EBM
Cr	850	7
K	130	1.7
Al	120	11
Cu	100	18
Fe	70	10
P	70	0.5
Cl	42	4
Si	17	17
Ca	13	5
Ni	8	5
Mg	4	0.7
Ti	3.5	1
Na	3	0.4
Zn	1.6	1
Mn	1.5	0.11

The concentrations of ^{232}Th and ^{238}U were measured by high resolution inductively Coupled plasma mass spectrometry (HR-ICP-MS), with a Thermo Fisher Scientific ELEMENT2 instrument. The sample was dissolved in acid solution and diluted for the measurement. A semiquantitative analysis was performed, i.e., the instrument was calibrated based on a single reference standard solution of ^{232}Th and ^{238}U. The results are shown in Table II. The signal for ^{238}U was close to background, which means that the calculated

TABLE II. Concentration of ^{232}Th and ^{238}U in the vanadium sample before purification obtained by HR-ICP-MS measurements with and without chromatographic extraction (EXC) of the analyses. The concentrations are given in units of 10^{-9} g/g. The estimated relative uncertainties are 30%.

Isotope	Without EXC	With EXC
^{232}Th	<0.5	<0.025
^{238}U	0.5	0.35

TABLE III. The isotopic composition of the vanadium sample in comparison with literature values [21].

Isotope	Abundance in % from [21]	Abundance in % from our samples
^{50}V	0.250 ± 0.004	0.239 ± 0.012
^{51}V	99.750 ± 0.004	99.761 ± 0.050

concentration for this isotope (in the first column of Table II) is affected by a large relative uncertainty (30%).

In order to have a more sensitive measurement of ^{232}Th and ^{238}U, another analysis of vanadium was performed, extracting and preconcentrating the analytes. Chromatographic extraction columns (EXCs) packed with U/TEVA® resins (Triskem International, France) were used for the selective extraction of thorium and uranium from vanadium after dissolution. As shown in Table II, the obtained results agree with those obtained from the first analysis. The reliability of the extraction procedure was confirmed by a recovery test: 80% recovery was found for both elements.

Additional ICP-MS measurements were carried out to confirm the isotopic composition of the vanadium sample, which could differ from the literature value, e.g., through extraction from different geological deposits. The measured isotopic abundances are shown in Table III and are consistent with the literature values. Hence, we have no evidence that the vanadium sample has an altered isotopic abundance and we proceed using the more precise literature value in the analysis.

B. Radiopurity of the vanadium sample

The initial and the purified metal sample were measured by means of γ-ray spectrometry with ultralow background high purity germanium (ULB-HPGe) detectors. The measurements were done in the STELLA (SubTerranean Low Level Assay) facility deep underground in the Gran Sasso National Laboratories of the INFN (Italy); details can be found in Refs. [22–26]. The sample of initial vanadium with a mass of 987.9 g in the form of small metallic flakes was placed in a polypropylene container in Marinelli geometry (GA-MA Associates, type 141G), above the end cap of the ULB-HPGe detector. This initial sample was measured for 35.3 d. After the purification by EBM, the vanadium was in the form of cylindrical ingots as shown in Fig. 2. The ingots were cut into ten disks and machined on the outside in order to obtain discs with equal diameter of 40 mm. A total sample mass of 818.5 g was obtained. The surface of the machined vanadium disks was purified by etching with a 0.1 molar solution of HNO_3. Each disk was sealed in a plastic bag. The measurement geometry of the final sample is shown in Fig. 3 and was optimized to yield the best detection efficiency and lowest self-absorption. The two largest disks (111.50 g and 115.60 g) were set on top of the inner part of a Marinelli beaker (type 141G), and the others were hung 87.5 mm from top of the outer wall on its inside around the end cap (75.95, 75.15, 75.14, 66.55, 73.80, 72.31, 76.45, and 76.02 g). The detection efficiencies for the full energy peaks in the sample-detector arrangement were obtained using the Monte Carlo (MC) simulation code MAGE [27], based on the GEANT4 software package.

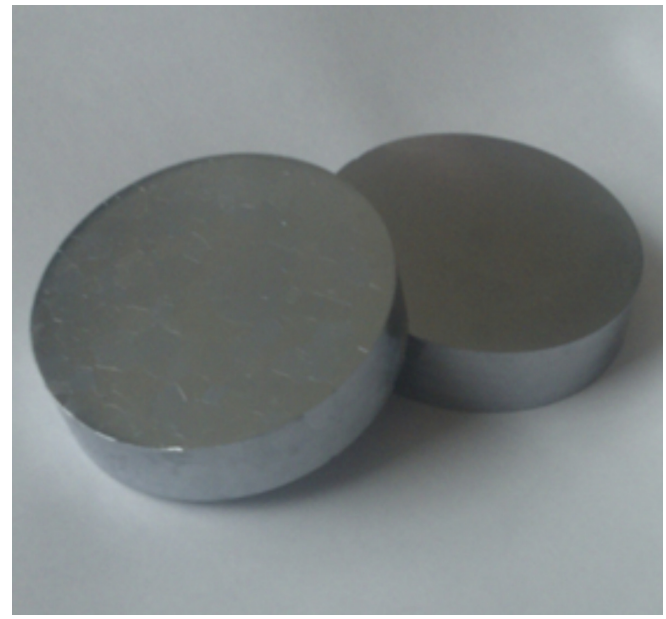

FIG. 2. Two vanadium discs after multifold electron beam melting (EBM).

The vanadium discs were measured after purification with an ULB-HPGe detector for 240.6 d. The spectrum is shown in Fig. 4 together with a 70.3 d background spectrum. The 1553.77 keV peak from the ^{50}V EC decay mode is clearly visible and is the most prominent feature in the source spectrum. Compton features of this γ ray dominate the background below the peak.

The measured activities of typical background isotopes before and after purification are given in Table IV. In both

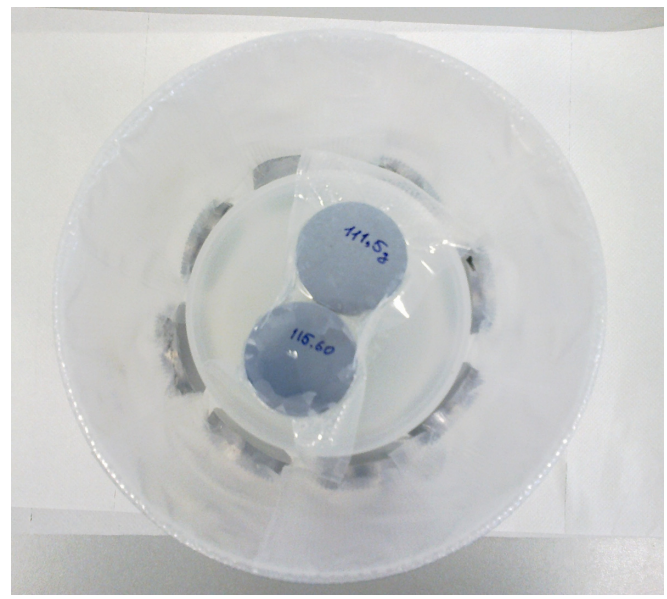

FIG. 3. Arrangement of the ten purified vanadium discs inside a Marinelli beaker ready to be measured.

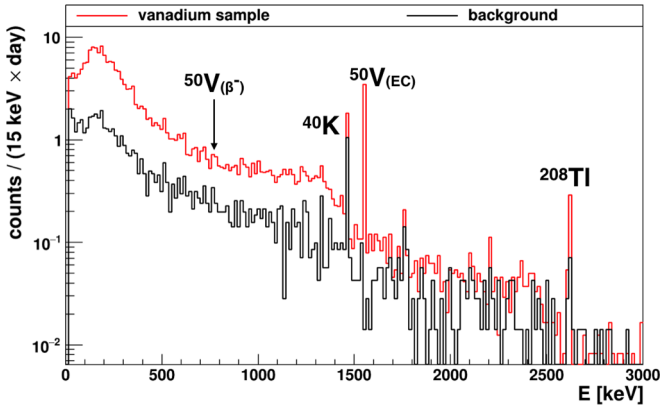

FIG. 4. Spectrum of the vanadium sample (240.6 d) in red and a corresponding background measurement (70.3 d) in black. Both spectra are scaled to live time. The two regions of interest and prominent background peaks are highlighted.

cases all observed peaks other than the one from ^{50}V EC are due to γ rays of the naturally occurring radioactivity coming from the U and Th chains, ^{40}K; from cosmogenic activation, ^{60}Co; and from man-made radioactivity, ^{137}Cs. As can be seen in Table IV, there is a significant reduction of the counting rate for all radionuclides after the purification. The activity of ^{40}K was reduced by a factor of 500. There has been also a significant reduction for the ^{238}U and ^{232}Th daughter nuclides, by a factor of 30 and 50, respectively. The background index in the region of interest for the ^{50}V β decay (783.29 keV) is reduced from 1.78 counts/(keV kg d) to 0.038 counts/(keV kg d), which enhances the experimental sensitivity by a factor of 7. In the vicinity of the 1553.77 keV γ line that is emitted in case of the ^{50}V EC, the background rate has been reduced from 0.172 counts/(keV kg d) to 0.00597 counts/(keV kg d), which improves the sensitivity by a factor of 5. A comparison between ICP-MS measurements and γ ray spectrometry for the vanadium samples before the purification shows that the secular equilibrium in both natural decay chains, uranium and thorium, was broken. This disequilibrium remains also in the γ-ray spectrometry results after the purification.

TABLE IV. The activity of radionuclides in the vanadium samples before and after purification, obtained by ULB-HPGe measurements. The measurement times are 35.3 and 240.6 d, respectively. Upper limits are given with 90% C.L., and the expanded standard uncertainties with $k = 1$.

Parent nuclide	A (mBq/kg) before	A (mBq/kg) after
^{228}Ra (^{232}Th)	41.3 ± 1.8	0.6 ± 0.1
^{228}Th (^{232}Th)	19.8 ± 0.8	0.4 ± 0.1
^{226}Ra (^{238}U)	14.5 ± 0.6	0.45 ± 0.05
^{234}Th (^{238}U)	<92.7	6 ± 2
^{234m}Pa (^{238}U)	<223	10 ± 3
^{235}U	4.2 ± 0.7	0.8 ± 0.1
^{40}K	3460 ± 170	7 ± 1
^{60}Co	0.8 ± 0.3	<0.1
^{137}Cs	<0.67	0.06 ± 0.02

III. ANALYSIS

The search is separated in two parts investigating the β^- and EC decay modes independently. The analysis is based on single γ-line peak fits at 783.29 and 1553.77 keV, respectively, including a semiempiric background model. The model is composed of a linear function in ± 20 keV around the peak of interest and known background γ lines within this region. Where possible, the strength of these background γ lines is constrained from more dominant γ lines elsewhere in the spectrum via prior information in a Bayesian concept.

The signal count s in the peak of interest is connected with the half-life $T_{1/2}$ of the decay mode as

$$s = \ln 2 \frac{1}{T_{1/2}} \epsilon N_A T m f \frac{1}{M}, \tag{1}$$

where ϵ is the full energy detection efficiency, N_A is the Avogadro constant, T is the live time (240.6 d), m is the mass of the vanadium sample (818.5 g), f is the natural isotopic abundance of ^{50}V (0.25%), and M the molar mass of natural vanadium (50.94). The Bayesian Analysis Toolkit (BAT) [28] is used to perform a maximum posterior fit. The likelihood $\mathcal{L}$ is defined as the product of the Poisson probabilities over each bin i for observing n_i events while expecting λ_i events:

$$\mathcal{L}(\mathbf{p}|\mathbf{n}) = \prod_i \frac{\lambda_i(\mathbf{p})^{n_i}}{n_i!} e^{-\lambda_i(\mathbf{p})}, \tag{2}$$

where $\mathbf{n}$ denotes the data and $\mathbf{p}$ the set of floating parameters. λ_i is taken as the integral of the extended probability distribution function $\mathcal{P}$ in this bin,

$$\lambda_i(\mathbf{p}) = \int_{\Delta E_i} \mathcal{P}(E|\mathbf{p}) dE, \tag{3}$$

where ΔE_i is the bin width. The counts in the fit region used to construct $\mathcal{P}$ are expected from (1) the Gaussian signal peak, (2) the linear background, and (3) a set of background peaks:

$$\begin{aligned} \mathcal{P}(E|\mathbf{p}) = & \frac{s}{\sqrt{2\pi}\sigma} \exp\left(-\frac{(E-E_0)^2}{2\sigma^2}\right) \\ & + B + C(E - E_0) \\ & + \sum_k \frac{b_k}{\sqrt{2\pi}\sigma} \exp\left(-\frac{(E-E_{b_k})^2}{2\sigma^2}\right). \end{aligned} \tag{4}$$

The first row describes the signal peak with the energy resolution σ and the γ-line energy E_0 as the mean of the Gaussian. The second row describes the linear background with the two parameters B and C. The third row describes the k background γ lines with the strength of the peak b_k. The specific background γ lines in the β^- and EC mode fit are described further below.

Each free parameter in the fit has a prior associated. The prior for the inverse half-life $(T_{1/2})^{-1}$ is flat. Priors for energy resolution, peak position, and detection efficiencies are Gaussian, centered around the mean values of these parameters. The width of these Gaussians is the uncertainty of the parameter values. This naturally includes the systematic uncertainty into the fit result.

The uncertainty of the peak positions is set to 0.1 keV. The energy scale and resolution are routinely determined using reference point sources including ^{228}Th and ^{152}Eu. The main γ lines of these radionuclides are fitted by a Gaussian distribution and the energy resolution is interpolated by a quadratic function. A resolution of $\sigma = 0.99$ keV was determined at 1553.77 keV with an estimated uncertainty of 5%. In the Bayesian framework, the posterior information of the resolution parameter in the fit to the prominent 1553.77 keV γ line can be used to update the knowledge of the detector resolution with *in situ* data. A posterior resolution of $\sigma = 0.92 \pm 0.02$ keV was determined which is used together with the standard calibration to inform the resolution prior for the β-decay mode fit. A σ of 0.73 ± 0.02 keV is used as prior on the resolution for the peak search at 783.29 keV.

The full energy peak detection efficiencies are determined with GEANT4 MC simulations tuned to a calibration standard in the same geometry as the vanadium sample. They are 2.69% at 783.29 keV and 1.94% at 1553.77 keV. A 5.0% uncertainty is assumed based on intercomparison tests and quality checks for single γ-ray emitters. Systematic uncertainties on the measured sample mass (0.01%), the isotopic abundance (1.6%), and the vanadium concentration in the sample (0.01%) enter the fit in the same way as the detection efficiency and yield a combined uncertainty on the efficiency parameter of 5.3%.

The posterior probability distribution is calculated from the likelihood and prior probabilities with BAT. The maximum of the posterior is the best fit. The posterior is marginalized for $(T_{1/2})^{-1}$, which is used to determine the 1σ uncertainties, defined as the smallest connected 68% probability region in the distribution. In case the probability distribution significantly includes zero, a lower half-life limit is set with the 90% quantile of the marginalized $(T_{1/2})^{-1}$ distribution equivalent to the 90% credibility interval (C.I.).

A. Analysis of β-decay mode

The fit is performed in the range between 763.3 and 803.3 keV. Seven known background γ lines are included in the fit even if they are not clearly visible in the spectrum. The selection is based on an emission probability above 1% or if the expected count rate is larger than 1 count in the dataset. The background γ lines are outlined in Table V.

The equilibrium of the ^{238}U decay chain was found to be broken at ^{226}Ra. The γ line of ^{234m}Pa at 1001.0 keV (0.84%) has 37.2 ± 9.1 counts, which was used together with their respective detection efficiencies to constrain the ^{234m}Pa γ lines at 785.96 and 785.4 keV. For the lower ^{238}U chain, the 609.3 keV γ line from ^{214}Bi (45.5%) with 45.2 ± 10.3 counts was used to constrain the 768.36 and 785.96 keV γ lines from ^{214}Bi and ^{214}Pb, respectively.

For the ^{232}Th chain, the average expectation from the 583.2 keV γ lines from ^{208}Tl (30.6%) with 52.1 ± 10.0 counts and from the 911.2 keV γ line from ^{228}Ac (25.8%) with 51.2 ± 9.9 counts was used to constrain the 794.95, 772.29, and 785.96 keV γ lines in the fit.

The best fit yields a positive signal at $T_{1/2}^{-1} = 2.27 \times 10^{-20}$ yr^{-1} or 4.4×10^{19} yr, which is distinct from the background-only hypothesis or 0 yr^{-1} by 1.2σ. Hence, no significant signal is observed and the 90% quantile of the marginalized $T_{1/2}^{-1}$ distribution yields 5.37×10^{-20} yr^{-1}. This translates into a lower half-life limit of

$$T_{1/2}(\beta^-) > 1.9 \times 10^{19}\text{yr (90\% C.I.)}.$$

The background below the peak is obtained from fit parameter B in Eq. (4) as 0.038 ± 0.002 counts/(kg d). The fit function is shown in Fig. 5, set to the best fit values (blue) and to the 90% limit of the signal process (red). Systematic uncertainties are included in the result but are negligible compared to the limit of low counting statistics. Fixing the peak position, resolution, and efficiency priors to their nominal values and repeating the fit without systematic uncertainty changes the limit by <0.2%. Choosing flat priors for the background γ lines instead of Gaussian constraints changes the limit by 4.1%.

This result is about one order of magnitude better than the one in Ref. [17] and approaches the theoretical prediction of 2×10^{19} yr in Ref. [18]. The obtained improvement is due to a factor of 7.9 more exposure and a factor of 3.2 lower background level. The analysis method differs with a full spectral fit compared to a counting method. The energy resolution and detection efficiency is similar in both searches. Also note that

TABLE V. Background γ lines in the β^--decay mode fit window with prior constrained based on more prominent background γ lines in their respective decay subchain. Note that the secular equilibrium of the ^{238}U decay chain is broken.

Nuclide	E (keV)	p_{emit} (%)	Prior counts	Constraining γ line
^{238}U chain				
^{234m}Pa	785.96	0.0544	2.9 ± 0.7	^{234m}Pa
^{234m}Pa	785.4	0.317	15.9 ± 4.0	^{234m}Pa
^{214}Bi	768.36	4.89	4.3 ± 1.0	^{214}Bi
^{214}Pb	785.96	1.06	1.1 ± 0.3	^{214}Bi
^{232}Th chain				
^{228}Ac	794.95	4.25	7.5 ± 1.5	^{208}Tl + ^{228}Ac
^{228}Ac	772.29	1.49	2.5 ± 0.5	^{208}Tl + ^{228}Ac
^{212}Bi	785.96	1.102	1.9 ± 0.4	^{208}Tl + ^{228}Ac

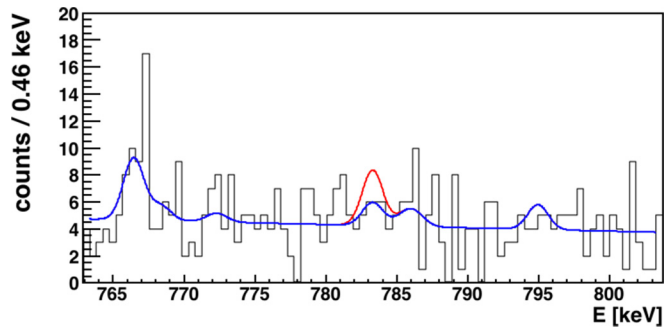

FIG. 5. Spectral fit of the ^{50}V β^- decay γ line at 783.29 keV and the background γ lines. Shown is the best fit function in blue and the signal process set to the obtained 90% C.I. limit in red.

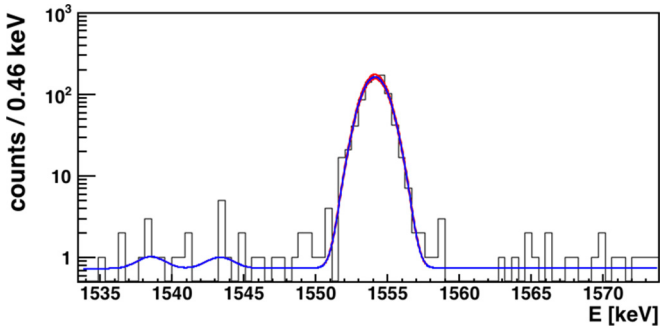

FIG. 6. Spectral fit of the ^{50}V EC γ line at 1553.77 keV and the background γ lines. Shown is the best fit function in blue and the signal process set to the $\pm 1\sigma$ fit uncertainties in red.

the limit in Ref. [17] is based on a 95% confidence level (C.L.) whereas this result quotes a 90% credibility interval (C.I.).

B. Analysis of electron capture mode

The EC γ line at 1553.77 keV is clearly visible in the spectrum (see Fig. 6, the best fit function in blue and the signal process set to the $\pm 1\sigma$ fit uncertainties in red). The fit range is chosen between 1533.8 and 1573.8 keV, including two background γ lines from ^{214}Bi at 1538.5 keV (0.40%) and at 1543.3 keV (0.30%). Constraints for these γ lines are again taken from the 1764.5 keV γ line from ^{214}Bi (32.7 ± 6.6 counts), resulting in an expectation of 1.4 ± 0.3 and 1.3 ± 0.3 counts, respectively. The expectation varies from the one based on the 609.3 keV γ line by about a factor of 5, which is likely due to ^{238}U background components in different locations that are not completely modeled in the MC simulation. This would result in different attenuation ratios between the two γ lines in data and MC simulation. Thus, the expectation is taken from the 1764.5 keV γ line which is closer in energy to the region of interest (ROI).

A γ line from ^{234m}Pa at 1553.75 keV (0.00821%) overlapping with the signal peak region was constrained with the more prominent γ line at 1001.0 keV to 0.3 counts and thus neglected.

The fit finds a best fit value at 2.67×10^{17} yr. The largest connected 68% interval in the marginalized $T_{1/2}^{-1}$ distribution is [2.49–2.83] $\times 10^{17}$ yr and taken as the uncertainty coming from the fit combining the statistical and systematic uncertainties naturally:

$$T_{1/2}(\mathrm{EC}) = 2.67^{+0.16}_{-0.18} \times 10^{17}\mathrm{yr}\ (68\%\ \mathrm{C.I.}).$$

This uncertainty is 6.4% of the best fit value and is dominated by the systematic contributions to the efficiency parameter as outlined in the uncertainty budget in Table VI. Switching off these systematic uncertainties in the fit, a range of [2.58–2.76] $\times 10^{17}$ yr is obtained, which corresponds to about 3.4% uncertainty composed of statistical and energy scale systematics combined. Changing the Gaussian priors for the background peaks to flat priors has no noticeable effect.

The measured half-life is about 14% higher and a factor 1.4 more precise compared to $2.29 \pm 0.25 \times 10^{17}$ yr previously reported in Ref. [17]. Both measurements agree within uncertainties.

TABLE VI. Uncertainty budget for the EC half-life measurement.

Uncertainty	Fraction in $T_{1/2}$
Isotopic abundance ^{50}V	1.6%
Vanadium concentration	0.1%
Sample mass	0.01%
Detection efficiency	5.0%
Subtotal	5.3%
Statistics and energy scale	3.5%
Fit total	6.3%

IV. CONCLUSIONS

The fourfold nonunique forbidden β decay and electron capture of ^{50}V have been investigated with a state-of-the-art ultralow background HPGe setup at LNGS, Italy. The half-life of the EC mode has been determined with unprecedented precision as $2.67^{+0.16}_{-0.18} \times 10^{17}$ yr (68% C.I.). The improvement could be achieved with about 10 times higher peak counts compared to a previous measurement, which renders the statistical uncertainty subdominant compared to systematic uncertainties. Future improvement can only be expected with a more sophisticated detector calibration or a detector setup with detection efficiency close to 1.

The half-life limit on the β-decay mode has been improved by more than an order of magnitude to 1.9×10^{19} yr (90% C.I.). The improvement was mainly possible due to a successful purification of the vanadium sample with electron beam melting in combination with the ultralow background detector deep underground. A longer measurement time and more sample mass compared the the previous best measurement also improved the limit. Both results are shown in comparison with previous measurements in Table VII. The half-life limit of the β-decay mode is at the point of theoretical predictions at 2.0×10^{19} yr. Even a modest improvement of the half-life sensitivity will either discover the decay or constrain nuclear model calculations. Further improvements with the setup at hand can be achieved with longer measuring time, more sample mass, or enrichment. A significant decrease of the background for the β-decay search is not easily feasible since the region around 783.3 keV is already dominated by the Compton features of the 1553.8 keV γ line coming from

TABLE VII. Measurements of ^{50}V decays in the last 45 years.

Mass (g)	Time (d)	$T_{1/2}^{EC}$ (10^{17} yr)	$T_{1/2}^{\beta^-}$ (10^{17} yr)	Ref., year
4000	48.88	>8.8	>7.0	[13], 1977
4250	135.5	$1.5^{+0.3}_{-0.7}$	>4.3	[14], 1984
100.6	8.054	$1.2^{+0.8}_{-0.4}$	>1.2	[15], 1985
337.5	46.21	2.05 ± 0.49	$8.2^{+13.1}_{-3.1}$	[16], 1989
255.8	97.8	2.29 ± 0.25	>15	[17], 2011
818.5	240.6	$2.67^{+0.16}_{-0.18}$	>190	this work

the EC mode of the same isotope. A conceptually different detector setup with active Compton detection would be required to reduce the background further.

Indeed, an approach using vanadium-based (YVO_4) crystals as cryogenic scintillating bolometers is discussed in Ref. [29]. First results of the crystal characterization show excellent bolometric performance and light output. An innovative approach for an efficient detection of the characteristic deexcitation γ rays following the ^{50}V β decay using triple coincidences, which yields experimental half-life sensitivities at the level of 10^{20} yr, is proposed as well. Therefore, the production of high radiopurity YVO_4 crystals from EBM purified vanadium which are operated as scintillating bolometers, read out with auxiliary light detectors, and surrounded by TeO_2 bolometers as Compton vetoes are considered as our further steps.

[1] H. Heiskanen, M. T. Mustonen, and J. Suhonen, J. Phys. G **34**, 837 (2007).
[2] J. Argyrlades *et al.*, Nucl. Phys. A **847**, 168 (2010).
[3] S. W. Finch and W. Tornow, Nucl. Instrum. Methods A **806**, 70 (2016).
[4] R. Arnold *et al.* (NEMO-3 Collaboration), Phys. Rev. D **93**, 112008 (2016).
[5] A. Bakalyarov *et al.*, Nucl. Phys. A **700**, 17 (2002).
[6] M. Huang *et al.*, Chin. Phys. C **41**, 030003 (2017).
[7] J. Heintze, Z. Naturforsch. A **10**, 77 (1955).
[8] R. N. Glover and D. E. Watt, Philos. Mag. **2**, 697 (1957).
[9] E. R. Bauminger and S. G. Cohen, Phys. Rev. **110**, 953 (1958).
[10] A. McNair, Philos. Mag. **6**, 559 (1961).
[11] D. E. Watt and R. L. G. Keith, Nucl. Phys. **29**, 648 (1962).
[12] C. Sonntag and K. O. Münnich, Z. Phys. **197**, 300 (1966).
[13] A. Pape, S. M. Refaei, and J. C. Sens, Phys. Rev. C **15**, 1937 (1977).
[14] D. E. Alburger, E. K. Warburton, and J. B. Cumming, Phys. Rev. C **29**, 2294 (1984).
[15] J. J. Simpson, P. Jagam, and A. A. Pilt, Phys. Rev. C **31**, 575 (1985).
[16] J. J. Simpson, P. Moorhouse, and P. Jagam, Phys. Rev. C **39**, 2367 (1989).
[17] H. Dombrowski, S. Neumaier, and K. Zuber, Phys. Rev. C **83**, 054322 (2011).
[18] M. Haaranen, P. C. Srivastava, J. Suhonen, and K. Zuber, Phys. Rev. C **90**, 044314 (2014).
[19] Yu. P. Bobrov *et al.*, Prob. At. Sci. Technol. **1**, 27 (2014).
[20] V. M. Azhazha *et al.*, Prob. At. Sci. Technol. **1**, 156 (2006).
[21] M. Berglund and M. E. Wieser, Pure Appl. Chem. **83**, 397 (2011).
[22] C. Arpesella, Appl. Radiat. Isot. **47**, 991 (1996).
[23] H. Neder, G. Heusser, and M. Laubenstein, Appl. Radiat. Isot. **53**, 191 (2000).
[24] G. Heusser, M. Laubenstein, and H. Neder, Radioact. Environ. **8**, 495 (2006).
[25] D. Budjas *et al.*, in *Proceedings of the XIV International Baksan School "Particles and Cosmology"*, Baksan Valley, Kabardino-Balkaria, Russia, April 16-21, 2007, edited by S. V. Demidov, V. A. Matveev, and V. A. Rubakov (2008), arXiv:0812.0768v1 [physics.ins-det].
[26] M. Laubenstein, Int. J. Mod. Phys. A **32**, 1743002 (2017).
[27] M. Boswell *et al.*, IEEE Trans. Nucl. Sci. **58**, 1212 (2011).
[28] A. Caldwell, D. Kollár, and K. Kröninger, Comput. Phys. Commun. **180**, 2197 (2009).
[29] L. Pattavina *et al.*, Eur. Phys. J. A **54**, 79 (2018).